

Characterization of Ge/SiGe strained-barrier quantum-well structures using photoreflectance spectroscopy

H. Yaguchi, K. Tai,* K. Takemasa, K. Onabe, and R. Ito

Department of Applied Physics, The University of Tokyo, 7-3-1 Hongo, Bunkyo-ku, Tokyo 113, Japan

Y. Shiraki

*Research Center for Advanced Science and Technology (RCAST), The University of Tokyo,
4-6-1 Komaba, Meguro-ku, Tokyo 153, Japan*

(Received 1 September 1993)

We have investigated Ge/SiGe strained-barrier quantum-well structures using photoreflectance spectroscopy. On the basis of the Γ -point transition energies associated with the Ge quantum well, the band offset at the heterojunction between Ge and SiGe has been found to vary linearly with the germanium composition in the SiGe barrier layer. The conduction-band-offset ratio $Q_c [= \Delta E_c / (\Delta E_c + \Delta E_{v,h})]$ at the Γ point is estimated to be 0.68 ± 0.08 . From the intrinsic linewidth of the quantum-well-related transitions, interface roughness has been characterized in this system and is estimated to be ± 1 monolayer in our samples.

I. INTRODUCTION

For heterostructure-based device applications, such as modulation-doped field-effect transistors (MODFET's), information about the heterointerface is of great importance. In particular, band offsets and interface roughness considerably affect device performance. In the SiGe system, the Ge/SiGe heterostructure is expected to be one of the most promising candidates for MODFET's,^{1,2} because the Ge channel is superior to the SiGe-alloy channel owing to its lighter effective mass and the absence of alloy scattering. In spite of the importance of the band offset and heterointerface roughness in the Ge/SiGe MODFET, they have not yet been adequately clarified, and there is some confusion in the existing data.

Several authors have studied the band offsets in the SiGe system experimentally³⁻⁵ or theoretically.^{6,7} For example, the valence-band offset at the Si/Ge heterointerface was estimated using x-ray photoemission spectroscopy of core levels.^{3,4} Photoemission spectroscopy, however, suffers from a considerable uncertainty in determining the valence-band-edge position relative to the core level. Rodrigues, Cerdeira, and Bean⁵ have taken advantage of photoreflectance (PR) to study quantum-confined direct transitions in Ge/Ge_{0.7}Si_{0.3} strained-layer superlattices, and obtained more reliable information about the band offsets at the heterojunction. In the present study, we have also employed the PR technique to investigate the band offsets at the Ge/SiGe heterointerface. In our experiment, however, single quantum-well (QW) structures have been used for precisely determining the band offsets. This is because single QW structures are expected to give less ambiguity than superlattices where interwell interactions induce level broadenings which can cause errors in the determination of the band offsets.

In III-V semiconductors, photoluminescence (PL) spectroscopy is often used for examining the height and

lateral size of islands at heterointerfaces.^{8,9} Although there have recently been many PL studies of SiGe QW structures, no investigation has been reported about the interface roughness using optical techniques in the SiGe system. This is because PL has been observed only from Si/SiGe QW's, in which the linewidth is determined mainly by alloy disorder rather than by interface roughness, and PL from Ge/SiGe QW structures has not yet been observed. In contrast to PL spectroscopy, PR spectroscopy can be used even for indirect-band-gap materials because it can detect direct optical transitions that are not at the lowest position in energy. In this study, therefore, we have characterized interface roughness in Ge/SiGe heterostructures utilizing the advantage of PR spectroscopy. To our knowledge, this is the first attempt to study the interface roughness in the SiGe system by an optical measurement. In order to estimate the interface roughness, we have deduced the intrinsic linewidth by measuring the temperature dependence of the PR spectra. From the quantum-number dependence of the intrinsic linewidth, the interface roughness has been estimated to be ± 1 monolayer (ML) at the Ge/SiGe heterointerface in our samples.

II. EXPERIMENTAL DETAILS

The samples used in this study were Ge/SiGe single strained-barrier quantum-well (SBQW) structures grown on Ge(100) substrates in a solid source Si molecular-beam epitaxy (MBE) system (VG Semicon V-80M) with a base pressure of 5×10^{-9} Pa. Germanium and silicon were evaporated with an effusion cell and an electron-beam gun, respectively. A *p*-type Ge substrate was cleaned using the following procedure after decreasing by organic solvents. The Ge substrate was first etched in a 10% H₂O₂ solution for 30 sec and rinsed in deionized water for 3 min. It was then dipped in a 5% HF solution for 10 sec

TABLE I. Sample used mainly for the determination of the band offset in this study. The structure was determined by double-crystal x-ray diffraction.

Sample	Well width (Å)	Barrier width (Å)	Ge composition in barrier layers
A	192	450	0.908
B	193	420	0.863
C	187	243	0.790

and rinsed in deionized water for 3 min. This procedure was repeated three times.

The chemically cleaned wafer was loaded into the growth chamber and heated at 800°C for 10 min to remove adsorbed gases and an oxide layer. Prior to the growth of a QW structure, a 900-Å-thick undoped Ge buffer layer was grown for smoothing the surface. The growth temperature ranged from 400 to 550°C. The growth rate was 1 Å/s. The pressure during the growth was lower than 10^{-7} Pa.

The structural parameters of the samples used mainly for the determination of the band offset are listed in Table I. In order to accurately determine the structure of the samples, we used the double-crystal x-ray diffraction technique. Cu $K\alpha_1$ ($\lambda=1.5406$ Å) line was used as an x-ray source. Ge(400) was used as the first crystal. Rocking curves were simulated based on the dynamical x-ray diffraction theory¹⁰ to determine the sample structure; that is, the well and barrier thicknesses and the Ge composition in the barrier layers. In this calculation, we used the parameters listed in Table II. We took the deviation¹¹ from Vegard's law into consideration for the determination of the SiGe alloy lattice constant as given in Table II. Furthermore, in the strained SiGe barrier layers, the lattice constant changes so as to accommodate the lattice mismatch between SiGe and Ge. In the case of the coherently strained $\text{Si}_{1-x}\text{Ge}_x$ layer grown on a Ge(100) substrate, the lattice constant perpendicular to the interface is given by

$$a_{\text{SiGe}}^{\perp} = a_{\text{SiGe}} \left[1 - \frac{2c_{12}}{c_{11}} \frac{a_{\text{Ge}} - a_{\text{SiGe}}}{a_{\text{SiGe}}} \right],$$

where a_{Ge} , a_{Si} , and a_{SiGe} are the lattice constants of unstrained Ge, Si, and SiGe, respectively. c_{11} and c_{12} are the elastic constants of $\text{Si}_{1-x}\text{Ge}_x$ which can be written as

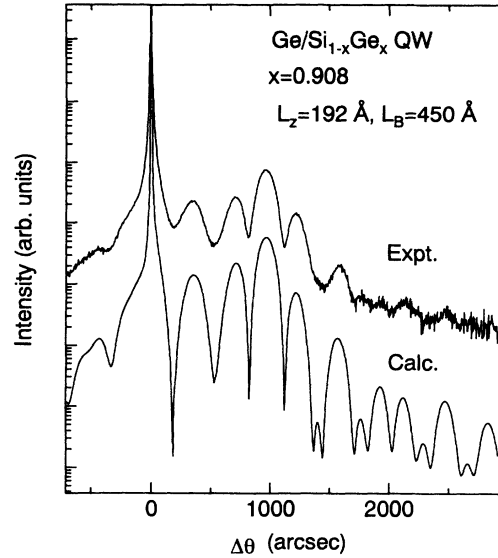


FIG. 1. X-ray-diffraction curves of a Ge/SiGe strained-barrier quantum-well structure. Upper and lower curves represent the experimental and simulated x-ray rocking curves, respectively.

$$c_{11} = \frac{xa_{\text{Ge}}c_{11}^{\text{Ge}} + (1-x)a_{\text{Si}}c_{11}^{\text{Si}}}{a_{\text{SiGe}}},$$

$$c_{12} = \frac{xa_{\text{Ge}}c_{12}^{\text{Ge}} + (1-x)a_{\text{Si}}c_{12}^{\text{Si}}}{a_{\text{SiGe}}},$$

where c_{ij}^{Ge} and c_{ij}^{Si} are the elastic constants of Ge and Si, respectively. For the x-ray atomic scattering factors, we adopted the analytical function calculated by Doyle and Turner¹⁴ based on the relativistic Hartree-Fock wave functions. In addition, we considered the dispersion corrections¹⁵ for the x-ray atomic scattering factors, $\Delta f'$ and $\Delta f''$, which are also listed in Table II. The linearly interpolated values were used for the x-ray atomic scattering factor of the SiGe alloy.

Figure 1 shows the typical experimental and simulated x-ray (400) rocking curves of a Ge/SiGe SBQW structure. In this sample, the well and barrier thicknesses and the Ge composition in the barrier layers are 192 Å, 450 Å, and 0.908, respectively. Roughly speaking, the peak position of the envelope is related to the germanium com-

TABLE II. Parameters used for the calculation of x-ray rocking curves.

Parameters	Ge	Si	$\text{Si}_{1-x}\text{Ge}_x$
a (Å)	5.6575 ^a	5.4310 ^a	$5.4310 + 0.1995x + 0.0270x^2$ ^b
c_{11} ($\times 10^{10}$ N/m ²)	12.40 ^c	16.577 ^d	see text
c_{12} ($\times 10^{10}$ N/m ²)	4.13 ^c	6.393 ^d	see text
$\Delta f'$	-1.163 ^e	0.244 ^e	linear interpolation
$\Delta f''$	0.886 ^e	0.330 ^e	linear interpolation

^aReference 11.

^bA quadratic equation was fitted to the results in Ref. 11.

^cReference 12.

^dReference 13.

^eReference 15.

position in the SiGe strained-barrier layers and the peak-to-peak spacing is inversely proportional to the sum of Ge well and SiGe barrier layer thicknesses. As shown in this figure, the simulated diffraction curve is in excellent agreement with the experimental data. This enabled us to determine the sample structure accurately, as listed in Table I.

The PR experimental setup used in this study was a conventional one. A monochromatic probe beam was obtained from white light of a 300-W halogen lamp using a 0.5-m monochromator (JASCO CT-50C, 600 lines/mm grating blazed at 1 μm). The slit width of the monochromator was set to 1 mm, which corresponded to the energy resolution higher than 2.5 meV. The reflected light from the sample was detected by an $\text{In}_x\text{Ga}_{1-x}\text{As}$ photodiode detector (New Focus 2011). To modulate the surface electric field in the sample, the 488-nm emission from an Ar-ion laser was used as a pump beam chopped at 800 Hz. A modulated signal was detected by a lock-in amplifier, and a dc signal was measured with a digital voltmeter. $\Delta R/R$ was derived by digitally dividing the ac signal by the dc signal. The PR measurements were carried out at temperatures between 4.2 and 300 K.

III. RESULTS AND DISCUSSION

We measured PR signals due to interband transitions at the Γ point in the Ge/SiGe SBQW structures. Figure 2 shows the band lineup at the Γ point in the Ge/SiGe SBQW structure. Since the SiGe barrier layers are under biaxial tensile strain, the electron–light-hole band gap becomes smaller than the electron–heavy-hole band gap. The band lineup of both heavy- and light-hole valence bands at the Γ point is of type I, as discussed below. The band offsets of the conduction, heavy-hole valence, and light-hole valence bands are defined as ΔE_c , ΔE_{vh} , and ΔE_{vl} , respectively, as indicated in Fig. 2.

Figure 3 shows a PR spectrum of a Ge/SiGe SBQW structure. The label $me-nhh$ (or $me-nlh$) shown in this figure denotes the transition between the m th conduction subband and the n th valence subband of the heavy-hole (hh) [or light-hole (lh)] character. Optical transitions related to the QW are distinctly observed, as well as transitions corresponding to the split band-gap energies of the strained SiGe barrier layer. Since the band-gap energies of the barrier layers are measured directly, the barrier

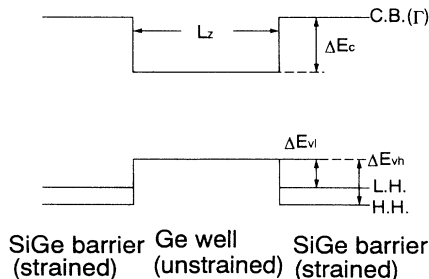


FIG. 2. Band lineup at the Γ point in a Ge/SiGe strained-barrier quantum-well structure.

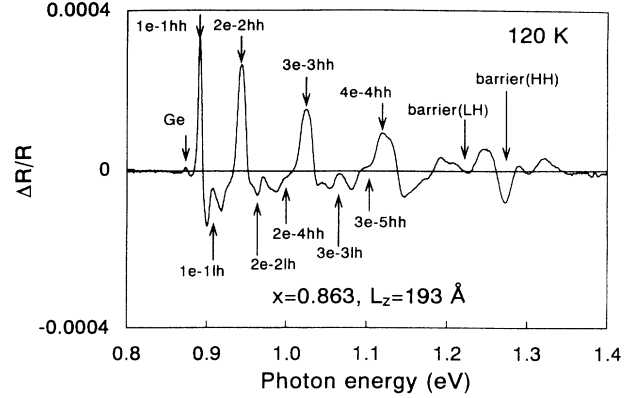


FIG. 3. PR spectrum of a Ge/SiGe strained-barrier quantum-well structure.

height can be determined accurately without using deformation potentials.

In order to derive optical transition energies from the PR spectra, first-derivative Lorentzian functions¹⁶ were fitted to the experimental data using the least-squares method. The transition energies obtained from the PR spectra of the Ge/SiGe SBQW structures measured at 80 K are listed in Table III. To determine the band offsets at the Ge/SiGe heterointerfaces, the calculated transition energies were compared with the experimental ones. Here, the heavy-hole-related transition energies were mainly used for determining the band offsets, because the

TABLE III. Transition energies obtained from PR spectra of Ge/SiGe strained-barrier quantum-well structures measured at 80 K. Theoretical values were calculated for the conduction-band-offset ratio $Q_c=0.68$. The nonparabolicity effect and the exciton effect are included in this calculation.

Sample	Transition	Experiment (eV)	Theory (eV)
A	Ge	0.887	
	1e-1hh	0.900	0.902
	2e-2hh	0.951	0.956
	3e-3hh	1.034	1.038
	barrier(lh)	1.126	
	barrier(hh)	1.168	
	B	Ge	0.887
1e-1hh		0.903	0.902
1e-1lh		0.915	0.907
2e-2hh		0.952	0.957
3e-3hh		1.035	1.043
4e-4hh		1.142	1.147
barrier(lh)		1.223	
barrier(hh)	1.273		
C	Ge	0.887	
	1e-1hh	0.901	0.904
	2e-2hh	0.958	0.963
	3e-3hh	1.050	1.057
	4e-4hh	1.163	1.171
	barrier(lh)	1.398	
	barrier(hh)	1.471	

TABLE IV. Parameters used in the calculation of quantum-well levels.

		Ge	Si	SiGe
electron effective mass	m_0^*	0.0380 ^a	0.64 ^b	linear interpolation
Luttinger parameters	γ_1	13.38 ^c	4.285 ^c	linear interpolation
	γ_2	4.24 ^c	0.339 ^c	linear interpolation

^aReference 17.^bReference 18.^cReference 19.

light-hole-related transitions were not observed as clearly as the heavy-hole-related ones. Moreover, since the light-hole states interact with the spin-orbit split-off states, the calculation of quantum-confined levels is more complicated. Table III also lists the transition energies calculated theoretically based on the envelope-function approximation. In this calculation, the nonparabolicity of the conduction band and the exciton binding energy have been considered, as discussed in detail below. The parameters used in this calculation are summarized in Table IV.

If the energy-independent electron effective mass is used for the calculation, the experimental transition energies are found always to be smaller than the calculated ones, especially in the higher-energy region, no matter what band offset value may be used. In addition, the number of transitions predicted theoretically is smaller than that observed experimentally in some cases. These are two possible reasons for these discrepancies. One is the smearing of the Ge composition in a QW owing to the segregation of Ge during the MBE growth.²⁰ In Ge-rich QW structures, however, Ge atoms prevent themselves from appreciable smearing,²¹ and hence it is unlikely that the potential shape of the QW changes so much as to cause the energy deviation from calculated values. The other possible reason is the nonparabolicity of the conduction band.^{22–26} Since the electron effective mass becomes heavier with increasing confinement energy, the actual energy levels may be lower than those calculated without considering the nonparabolicity effect. We incorporated the nonparabolicity of the conduction band through the expression²⁴

$$m^*(E) = m_0^*(1 + \alpha E),$$

where m_0^* is the electron effective mass at $k=0$, α is the nonparabolicity parameter, and E is the confinement energy. The nonparabolicity was considered only for the Ge well layer because the transition energy is little affected by possible changes in the effective mass in the barrier layer. In this study, α was treated as a fitting parameter, since it is not well known. The best fit was obtained for all the samples with $\alpha = 1.25 \text{ eV}^{-1}$. For GaAs, it was reported that $\alpha = 0.642 \text{ eV}^{-1}$.²⁴ Therefore, the nonparabolicity effect is more important in the Ge/SiGe QW structures than in GaAs-related QW structures. The value of our nonparabolicity parameter is even larger than that assumed for the Ge/Ge_{0.7}Si_{0.3} superlattices by Rodrigues, Cerdeira, and Bean;⁵ $\alpha = 0.92 \text{ eV}^{-1}$, which was calculated based on the Kane model.²⁷ Nevertheless,

it should be emphasized that the nonparabolicity effect is extremely important when the quantum levels in Ge/SiGe QW's are treated.

Since the transition observed by PR measurements in this study are excitonic, the exciton binding energy should also be taken into account. Using the simple analytical method presented by Mathieu, Lefebvre, and Christol,²⁸ the exciton binding energy was estimated as 4 meV for a 200-Å-wide Ge/Si_{0.2}Ge_{0.8} QW. Thus all the QW-related transition energies given in Table III were derived by subtracting 4 meV from the calculated values, neglecting the dependence on the Ge composition and the quantum number for simplicity.

On the basis of the comparison between experimental and theoretical transition energies, we have determined the band offsets at the heterojunction and their dependence on the germanium composition. The results are shown in Fig. 4. It can be seen that the band lineup of both heavy- and light-hole valence bands at the Γ point is of type I at the heterojunction between a strained SiGe layer and an unstrained Ge layer. In addition, it is found

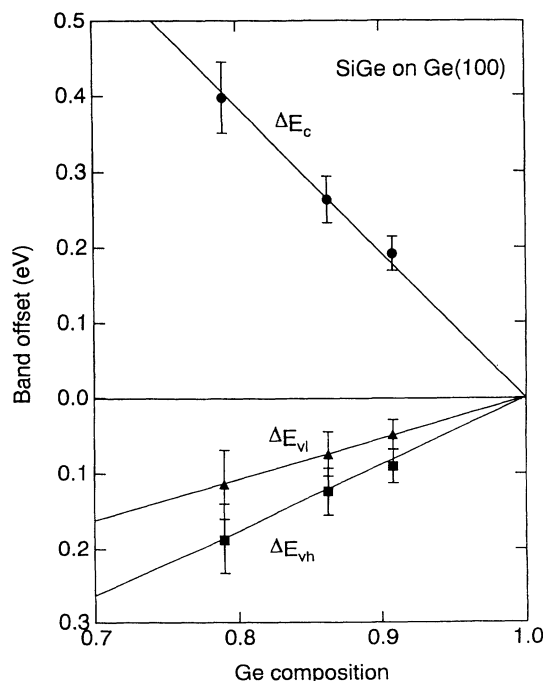


FIG. 4. Band offsets at the heterointerface in Ge/SiGe strained-barrier quantum-well structures.

that the band offsets are almost linearly dependent on the Ge composition. In other words, the average valence-band offset varies linearly with the Ge composition, which is consistent with a theoretical precision.⁶ The conduction-band-offset ratio Q_c [$=\Delta E_c/(\Delta E_c + \Delta E_{vh})$], defined in the same way as in Ref. 5, is found to be 0.68 ± 0.08 in the region $x > 0.7$. The possible errors arise primarily because the calculated transition energies unfortunately become maximum around $Q_c = 0.7$. If the Ge composition in the barrier layer is extrapolated to $x = 0$ (i.e., Si), the light-hole valence-band offset becomes $\Delta E_{vl} = 0.52 \pm 0.22$ eV.

Let us compare our results with other studies concerning the band offsets in the Ge/SiGe heterostructures. Van de Walle and Martin⁶ calculated the band offset at the heterojunction between strained Si and unstrained Ge based on a model-solid theory and determined $\Delta E_{vl} = 0.31 \pm 0.2$ eV. Schwartz *et al.*³ reported $\Delta E_{vl} = 0.17 \pm 0.13$ eV based on photoemission spectroscopy of core levels. Yu, Crobe, and McGill⁴ also used photoemission spectroscopy to study the valence-band offset and determined $\Delta E_{vl} = 0.22 \pm 0.13$ eV. On the other hand, using PR spectroscopy, Rodrigues, Cerdera, and Bean⁵ reported $Q_c = 0.73 \pm 0.03$, which corresponds to $\Delta E_{vl} = 0.32 \pm 0.08$ eV at the Si/Ge(001) interface. In our study, the estimated light-hole valence-band offset is larger than that obtained by other studies. In particular, the values obtained from photoemission measurements are considerably smaller than our result. The large discrepancy is probably due to the surface segregation of Ge atoms which smears the interfacial abruptness.²⁰ Ge surface segregation may also account for the observation that for Ge on Si(100) the experimental value³ is in good agreement with theory,⁶ but that for Si on Ge(100) the agreement is not as good. This is because, although Ge atoms segregate while Si is deposited on Ge substrates, Si atoms do not segregate while Ge is deposited on Si substrates due to the surface potential-energy difference. The result of Rodrigues, Cerdeira, and Bean⁵ is relatively close to our result. However, they used Ge/Ge_{0.7}Si_{0.3} strained-layer superlattices to determine the band offset. In the superlattice, interwell interactions produce level broadenings and miniband formation which can cause ambiguity in the determination of the transition energies. On the other hand, in the case of Ge/SiGe single SBQW structures used in our study, the calculation of the confined levels is straightforward and there is no ambiguity in this respect. The differences in the experimental values of the conduction-band-offset ratio, therefore, have probably resulted from the difference in the sample structure or the difference in the nonparabolicity parameter used in the calculation.

In order to consider the interface roughness at the heterojunction, we have focused our attention on the linewidth of the optical transitions. The intrinsic linewidth was estimated from the temperature dependence of the linewidth of the QW-related transitions. Figures 5 and 6 show the temperature dependence of the PR spectra and the linewidth of heavy-hole-related transitions, respectively. Since the linewidth does not always become narrower with decreasing temperature, the

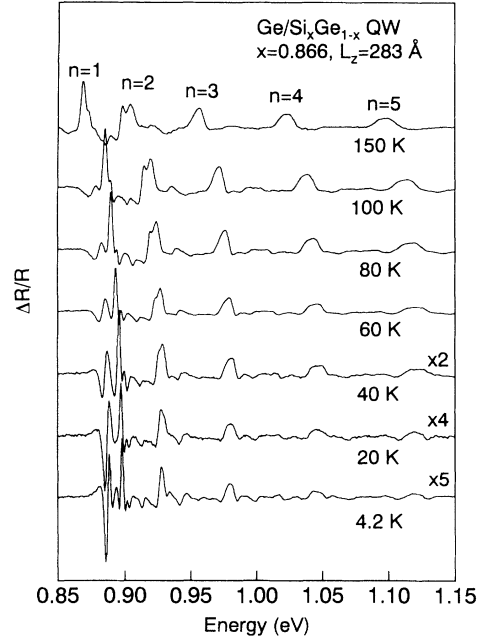


FIG. 5. Temperature dependence of the PR spectra of a Ge/SiGe strained-barrier quantum-well structure.

minimum linewidth in the measured temperature range has been taken to be the intrinsic linewidth. If the intrinsic linewidth originates mainly from interface roughness and alloy disorder in the SiGe barrier layers, the intrinsic broadening parameter can be expressed as

$$\Gamma_0 = \left[\frac{\partial E}{\partial L_z} \right]_x \Delta L_z + \left[\frac{\partial E}{\partial x} \right]_{L_z} \Delta x .$$

The first and second terms represent the contributions of the interface roughness and alloy disorder, respectively. We have found that the contribution of the interface roughness is much larger than that of alloy disorder.

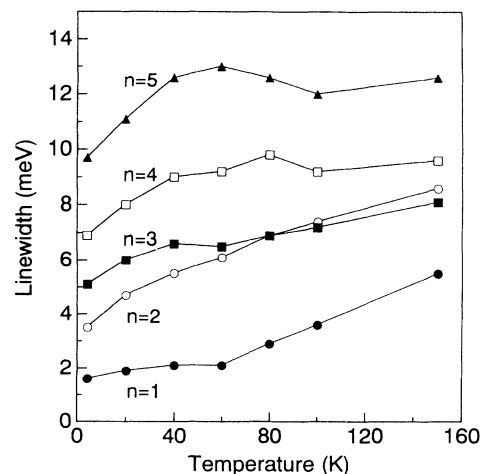


FIG. 6. Temperature dependence of the linewidth of heavy-hole-related transitions in a Ge/SiGe strained-barrier quantum-well structure.

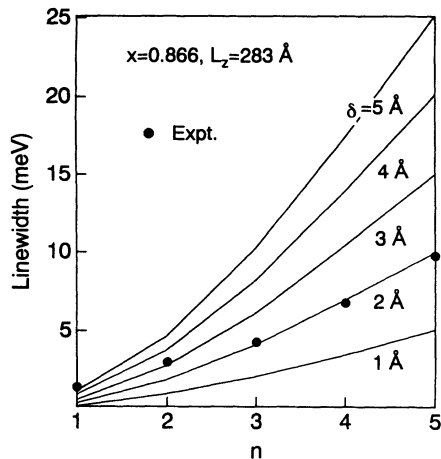


FIG. 7. Quantum-number dependence of the intrinsic linewidth of heavy-hole-related transitions. Solid lines are calculated for various fluctuations in the well width.

Therefore, it is appropriate to treat the interface roughness as the main cause in determining the linewidth broadening. In addition to the temperature dependence, it is apparent in Fig. 5 that the linewidth becomes broader with increasing quantum number.

In Fig. 7, we show the quantum-number dependence of the intrinsic linewidth. Since the samples used in this study are single QW structures, there is no possibility of interwell fluctuations, and only intrawell fluctuations cause the broadening. As is seen in this figure, the quantum-number dependence agrees well with the calculation if the interface roughness is assumed to be 2 Å. The interface roughness of 1.5~2 Å was also obtained in

other samples. That is, the roughness at the Ge/SiGe heterointerface is estimated to be ± 1 ML in our samples. A small deviation at small quantum numbers is probably due to the experimental resolution of our PR system. In the estimation of the interface roughness, the lateral size of the islands was assumed to be comparable to the exciton Bohr radius (~ 200 Å) according to the model of Singh, Bajaj, and Chaudhuri.⁹ If the lateral size of the islands were larger than the Bohr radius, splittings would be observed in the PR spectra. If the island size were smaller than the Bohr radius,⁹ on the other hand, the linewidth would be much narrower than we have observed.

IV. CONCLUSIONS

We have investigated Ge/SiGe SBQW structures using PR spectroscopy. On the basis of the QW-related transition energies, the band offsets at the Γ point were evaluated. The conduction-band-offset ratio was found to be 0.68 ± 0.08 . From the intrinsic linewidth, the interface roughness at the Ge/SiGe heterointerface was characterized. The height of the islands was about 1 ML, and their lateral dimensions were comparable to the exciton Bohr radius.

ACKNOWLEDGMENTS

We would like to acknowledge the discussion of photoreflectance spectroscopy with Professor C. Hamaguchi. We would like to thank Dr. S. Koshiba for his assistance in the x-ray-diffraction measurements. We also would like to thank Dr. S. Fukatsu for his valuable advice, and S. Ohtake for his technical assistance.

*Present address: Oki Electric Industry Co., Ltd., 550-1 Higashiasakawa, Hachioji, Tokyo 193, Japan.

¹G. R. Wagner and M. A. Janocko, *Appl. Phys. Lett.* **54**, 66 (1988).

²H. Etoh, E. Murakami, A. Nishida, K. Nakagawa, and M. Miyao, *Jpn. J. Appl. Phys.* **30**, L163 (1991).

³G. P. Schwartz, M. S. Hybertsen, J. Bevk, R. G. Nuzzo, J. P. Mannaerts, and G. J. Gualtieri, *Phys. Rev. B* **39**, 1235 (1989).

⁴E. T. Yu, E. T. Croke, and T. C. McGill, *Appl. Phys. Lett.* **56**, 569 (1990).

⁵P. A. M. Rodrigues, F. Cerdeira, and J. C. Bean, *Phys. Rev. B* **46**, 15 263 (1992).

⁶C. G. Van de Walle and R. M. Martin, *Phys. Rev. B* **34**, 5621 (1986).

⁷L. Colombo, R. Resta, and S. Baroni, *Phys. Rev. B* **44**, 5572 (1991).

⁸C. Weisbuch, R. Dingle, A. C. Gossard, and W. Weigmann, *J. Vac. Sci. Technol.* **17**, 1128 (1980).

⁹J. Singh, K. K. Bajaj, and S. Chaudhuri, *Appl. Phys. Lett.* **44**, 805 (1984).

¹⁰M. A. G. Haliwell, M. H. Lyons, and M. J. Hill, *J. Cryst. Growth* **68**, 3021 (1964).

¹¹J. P. Dismukes, L. Ekstrom, and R. J. Paff, *J. Phys. Chem.* **68**, 3021 (1964).

¹²Y. A. Burenkov, S. P. Nikanorov, and A. V. Stepanov, *Fiz. Tverd. Tela (Leningrad)* **12**, 2428 (1970) [*Sov. Phys. Solid State* **12**, 1940 (1971)].

¹³H. J. McSkimin and P. Andreatch, Jr., *J. Appl. Phys.* **35**, 2161 (1964).

¹⁴P. A. Doyle and P. S. Turner, *Acta Crystallogr. Sec. A* **24**, 390 (1968).

¹⁵*International Tables for X-Ray Crystallography* (Kyonoch, Birmingham, 1974), Vol. 4.

¹⁶B. V. Shanabrook, O. J. Glembocki, and W. T. Beard, *Phys. Rev. B* **35**, 2540 (1987).

¹⁷R. L. Aggarwal, *Phys. Rev. B* **2**, 446 (1970).

¹⁸R. People and S. A. Jackson, *Phys. Rev. B* **36**, 1310 (1987).

¹⁹O. Madelung, in *Intrinsic Properties of Group IV Elements and III-V, II-VI and I-VII Compounds*, edited by O. Madelung, Landolt-Börnstein, New Series, Group X, Vol. 22, Pt. a (Springer-Verlag, Berlin, 1987).

²⁰K. Fujita, S. Fukatsu, H. Yaguchi, Y. Shiraki, and R. Ito, *Appl. Phys. Lett.* **59**, 2240 (1991).

²¹S. Fukatsu, K. Fujita, H. Yaguchi, Y. Shiraki, and R. Ito, *Appl. Phys. Lett.* **59**, 2103 (1991).

²²U. Rössler, *Solid State Commun.* **49**, 943 (1984).

²³M. Braun and U. Rössler, *J. Phys. C* **18**, 3365 (1985).

²⁴U. Ekenberg, *Phys. Rev. B* **40**, 7714 (1989).

²⁵T. Ruf and M. Cardona, *Phys. Rev. B* **41**, 10 747 (1990).

²⁶R. People and S. K. Sputz, *Phys. Rev. B* **41**, 8431 (1990).

²⁷E. O. Kane, *J. Phys. Chem. Solids* **1**, 249 (1957).

²⁸H. Mathieu, P. Lefebvre, and P. Christol, *Phys. Rev. B* **46**, 4092 (1992).